

## Magnetic properties of single crystals of $\text{GdCo}_2$ , $\text{HoNi}_2$ , and $\text{HoCo}_2$

D. Gignoux, F. Givord, and R. Lemaire

*Laboratoire de Magnétisme, Centre National de la Recherche Scientifique, B.P. 166, 38042 Grenoble Cedex, France*

(Received 25 November 1974)

Magnetic measurements which have been performed on single crystals of the  $\text{GdCo}_2$ ,  $\text{HoNi}_2$ , and  $\text{HoCo}_2$  Laves phases lead to a quantitative analysis of the crystal-field effects on energy and magnetization anisotropies. The anisotropy due to cobalt is negligible. Crystal-field parameters have been determined from the magnetization variation in intense magnetic fields. The change of easy magnetization direction observed at 14 K on  $\text{HoCo}_2$  corresponds to a change, with temperature, of the level scheme of the  $^5J_8$  ground-state multiplet. An entropy discontinuity is associated with this transition, leading to a specific-heat anomaly. For  $\text{HoCo}_2$ , the values of the anisotropy constants at 0 K are  $K_1 = -10^7$  erg/cm<sup>3</sup> and  $K_2 = 10^9$  erg/cm<sup>3</sup>. The interactions in  $\text{HoNi}_2$  are weak compared to crystal-field effects; when a magnetic field is applied, the anisotropy increases so much that it is no longer possible to measure it.

### I. INTRODUCTION

In the rare-earth (*R*) cobalt-rich compounds with a structure derived from the  $\text{CaCu}_5$ -type structure by means of substitutions, the cobalt magnetic moment decreases when the percentage of rare earth alloyed is increased. This effect is due to the progressive filling of the  $3d$  band and is very strong in the  $R\text{Co}_2$  cubic Laves phases.<sup>1,2</sup>

The analogy between the magnetic properties of  $\text{YCo}_2$  and palladium has been noted in 1968.<sup>3</sup> The first-order transition of  $\text{HoCo}_2$  was associated with exchange effects due to holmium atoms, which induce a magnetic moment of  $1\mu_B$  per cobalt atom. More recently, a quantitative interpretation of these phenomena in a collective electrons model was given.<sup>4</sup>

Single crystals have been prepared in order to obtain information on magnetization mechanisms and especially to determine magnetic-moment density maps by means of polarized-neutron diffraction. Only results of magnetization measurements performed on  $\text{GdCo}_2$ ,  $\text{HoNi}_2$ , and  $\text{HoCo}_2$  along the three principal symmetry directions will be presented in this paper. These compounds were chosen to clarify the particular thermal variation of the  $\text{HoCo}_2$  magnetization: the magnetization measured under 5 kOe on a polycrystalline sample exhibits a maximum near 14 K.<sup>2</sup> Around this temperature, the thermal variation of the specific heat also shows a maximum.<sup>4</sup> This anomaly has been attributed to a strong temperature dependence of the magnetocrystalline anisotropy. The study of  $\text{GdCo}_2$  and  $\text{HoNi}_2$  gives information on the respective cobalt and holmium contributions to the magnetocrystalline anisotropy: in  $\text{GdCo}_2$ , gadolinium, as an *S* state, does not contribute to the anisotropy; in the ferromagnetic  $\text{HoNi}_2$  com-

pound, nickel is not magnetic and holmium only contributes to the anisotropy.  $\text{GdCo}_2$  and  $\text{HoCo}_2$  are ferrimagnetic; a  $1\mu_B$  moment per cobalt atom is coupled antiparallel to the moment of gadolinium or holmium atoms.

### II. SINGLE-CRYSTAL PREPARATION AND EXPERIMENTAL TECHNIQUES

Two methods were used to prepare the single crystals. In the first one, the melted alloy is slowly cooled down (20 K per hour around solidification temperature). In the second one, a temperature-gradient furnace of the Bridgman type was used.<sup>5</sup> Polycrystalline samples were first prepared in a levitation furnace from 99.9%-pure constituents. In the single-crystal furnace, these were put into conically shaped crucibles made of recrystallized alumina. The first method, which is quicker, decreases the reaction between sample and crucible. The Curie temperature is very sensitive to small amounts of aluminium in the compound. With this method, we have been able to prepare single crystals with Curie temperatures identical to those of polycrystalline samples prepared in the levitation furnace and then annealed at 900 °C. The first-order Curie temperature of  $\text{HoCo}_2$  is thus perfectly defined at 78 K.

In order to take into account demagnetizing field effects, the single crystals have been spark cut into 3-mm-diam spheres. Magnetization measurements were performed at the Service National des Champs Intenses of Grenoble in fields up to 130 kOe and in a temperature range from 1.4 to 300 K.

Magnetic anisotropy was determined by measuring the energies needed to magnetize a single crystal along several crystallographic directions.

In fact, the variation of a crystal magnetization with the applied magnetic field depends on the field direction. Figure 1 shows the magnetization variations (e) and Abd when the field is applied in the easy-magnetization direction and in a difficult one, respectively. For the value  $H_0$  of the internal field, magnetization becomes parallel to the difficult-magnetization direction. The weak line Bb represents the magnetization variation if it remains parallel to the difficult-magnetization direction. The AbB triangle area represents the free-energy difference between the A state, with the magnetization  $M_e$  parallel to the easy-magnetization direction, and the B state with the magnetization  $M_d$  parallel to the difficult-magnetization direction. This area gives the energy anisotropy value. The difference between the two (e) and Bbd curves represents the magnetization anisotropy, which depends on the magnetic field. For a cubic compound, the free energy in one direction with  $\alpha_1, \alpha_2, \alpha_3$  direction cosines may be written as a function of the  $K_1$  and  $K_2$  anisotropy constants,

$$F = K_0 + K_1(\alpha_1^2\alpha_2^2 + \alpha_2^2\alpha_3^2 + \alpha_1^2\alpha_3^2) + K_2\alpha_1^2\alpha_2^2\alpha_3^2,$$

which leads to

$$F[110] - F[100] = \frac{1}{4}K_1,$$

and

$$F[111] - F[100] = \frac{1}{3}(K_1 + \frac{1}{9}K_2).$$

### III. RESULTS

#### A. GdCo<sub>2</sub>

The measured GdCo<sub>2</sub> sphere is not a perfect single crystal: 80% of the sample consists of a large single crystalline dendrite. The intermediate space is filled with polycrystalline Gd<sub>2</sub>Co<sub>3</sub> neighboring phase. The sample magnetization under 100 Oe exhibits a strong decrease at 400 K, the GdCo<sub>2</sub> Curie temperature. Magnetization under high fields was measured at 4.2 K along the three principal axes. The easy magnetization direction is the [100] axis. Energy anisotropy is very weak: free-energy differences between the [110] and [100] axes and between the [111] and [100] axes have similar values, which are about  $2 \cdot 10^5$  erg/cm<sup>3</sup> at 4.2 K. Within the experimental accuracy, magnetization anisotropy is negligible. The spontaneous magnetization value at 4.2 K is  $5.3 \mu_B$  per GdCo<sub>2</sub> formula. This value is higher than those obtained with pure GdCo<sub>2</sub> polycrystalline samples ( $4.9 \mu_B$ ) because the Gd<sub>2</sub>Co<sub>3</sub> magnetization is larger than that of GdCo<sub>2</sub>, which is less rich in gadolinium. However, this measurement allowed us to estimate the cobalt magnetocrystalline anisotropy in the RCo<sub>2</sub> compounds,

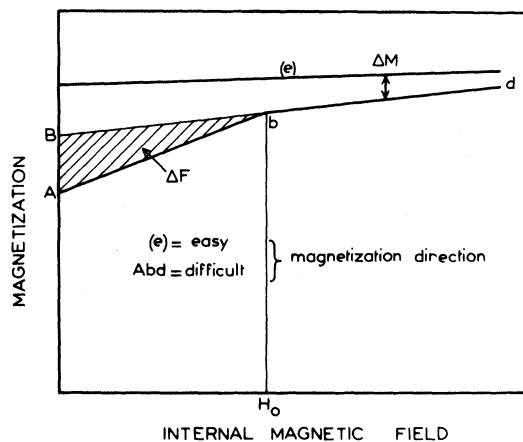


FIG. 1. Variation of the magnetization of a cubic single crystal with the magnetic field applied along the easy-magnetization direction and along a difficult one.

which must be smaller than that found for GdCo<sub>2</sub>.

#### B. HoNi<sub>2</sub>

The magnetization in a 100-Oe field applied along the [100] direction decreases rapidly at about 13 K; the inflection point has been taken as the ferromagnetic Curie temperature of HoNi<sub>2</sub>  $T_c = 13.4$  K. In the paramagnetic state, magnetization varies linearly with weak fields, and the reciprocal susceptibility follows a Cuire-Weiss law

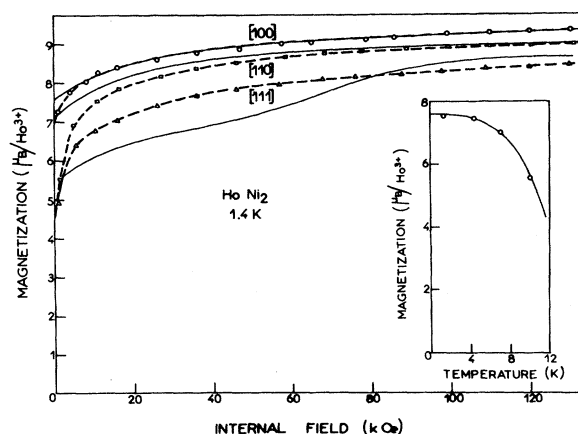


FIG. 2. Magnetization variation of HoNi<sub>2</sub> at 1.4 K as a function of internal field; the internal field is deduced from the applied field by subtracting the demagnetizing field which is uniform with the value  $(4\pi/3)M$  for the measured spherical specimen. Experimental points are connected by a dashed line. Full lines represent the magnetization variation calculated with the parameters  $x = -0.50$ ,  $W = 0.62$  K, and  $\alpha = 4.0$  K, when field and magnetization are parallel. The insert shows the comparison between experimental and calculated values of the spontaneous magnetization.

corresponding to the free  $\text{Ho}^{3+}$  ion. The paramagnetic Curie temperature was found to be  $\Theta_p = 16$  K, in good agreement with previous results obtained on polycrystals.<sup>6,7</sup> The good crystallization of the sample explains the lower value found for the ferromagnetic Curie temperature: stacking faults are more numerous in a polycrystalline sample, especially if reduced to a powder, and tend to increase the ordering temperature.<sup>8</sup> Figure 2 shows the magnetization at 1.4 K versus the internal magnetic field measured along the three principal symmetry axes. The easy-magnetization direction is [100]. The spontaneous-magnetization value, obtained at zero internal field, is  $7.55\mu_B$  per formula, the values measured along the [110] and [111] directions being, respectively,  $5.34\mu_B$  and  $4.33\mu_B$ , in good agreement with the phase rule.<sup>9</sup> Magnetization variations at 4.2, 7, and 10 K are similar to those at 1.4 K. Along the difficult-magnetization direction, the curves do not show the break characteristic of the field value for which magnetization has become parallel to the field. It is therefore impossible to separate energy anisotropy from magnetization anisotropy.

### C. $\text{HoCo}_2$

The magnetization in a 100-Oe field applied along the [100] direction decreases abruptly at 78 K, as shown in Fig. 3; the hysteresis of the first-order transition is 2 K. In the paramagnetic state, the magnetization variation with the applied field shows a transition between 78 and 90 K. The critical-field value and its variation with temperature are nearly independent of the applied-field direction and are similar to those measured on polycrystalline samples.<sup>2</sup> The thermal variations of the reciprocal paramagnetic susceptibility along the three directions are identical and are in perfect agreement with that previously determined for polycrystalline samples.<sup>10</sup>

A change of easy-magnetization direction is observed at 14 K. The spontaneous magnetization, which is parallel to the [110] direction at very low temperatures, becomes parallel to the [100] direction when temperature increases (Fig. 4). For zero internal fields, the phase rule is observed except around the transition temperature at which, as shown by the magnetization variation at 14.4 K, the plane (100) is of easy magnetization. At all temperatures below the Curie temperature, the free-energy difference between the [100] and [110] directions and the magnetization anisotropy may be obtained by comparing the magnetizations measured along these two directions. The break observed at the field  $H_1$  on the magnetization curves along [100] for  $T < 14$  K and along [110]  $T > 14$  K

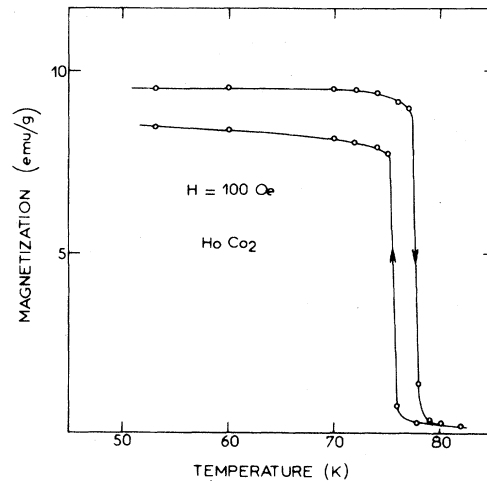


FIG. 3. Determination of the first-order  $\text{HoCo}_2$  Curie temperature from the thermal variation of magnetization in a 100-Oe field applied parallel to the [100] direction.

corresponds to the magnetization alignment parallel to the field. In higher fields, the field dependence of magnetization becomes linear. It corresponds mainly to the energy-level purification by the field. The field effects on the conduction band and on  $3d$  electrons are weaker, the  $\text{YCo}_2$  susceptibility<sup>2</sup> being only about  $10^{-5}$  emu/g. Magnetization anisotropy was measured under a 100-kOe applied field. Energy anisotropy values are obtained from the shaded areas on Fig. 4. Experimental points are shown in Figs. 5 and 6. Magnetization anisotropy exhibits a minimum at 25 K, while energy anisotropy is maximum at 40 K. At 14 K,  $K_1$  changes sign.

Above 14 K, the magnetization curves measured along the [111] direction (Fig. 4) show a break for a field  $H_2 \approx H_1 / \cos \alpha$  with  $\alpha = 35^\circ$ , the value of the angle between the [111] and [110] directions. The free-energy difference between the [100] and [111] directions is much larger than that between the [100] and [110] ones, and the effect of a field below  $H_2$ , applied along the [111] direction, is mainly to rotate the magnetization inside the (100) plane towards the [110] direction. Below 14 K, the easy-magnetization axis being [110], the curves do not show such a break.

### IV. DISCUSSION

The high magnetic-energy anisotropy and high magnetization anisotropy observed in  $\text{HoNi}_2$  and  $\text{HoCo}_2$ , as well as the change of the easy-magnetization direction of  $\text{HoCo}_2$ , can be attributed to crystal-field effects on the  $4f$  electrons of the  $\text{Ho}^{3+}$  ions. The perturbing Hamiltonian acting on

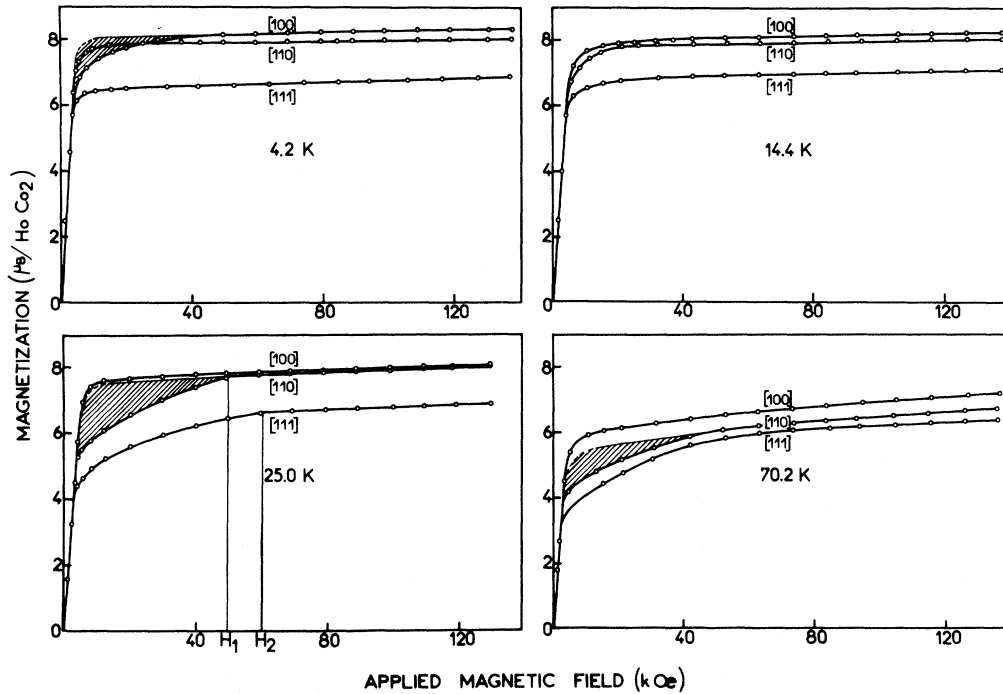


FIG. 4.  $\text{HoCo}_2$  magnetization variations with field applied along the three principal symmetry directions. The weak lines represent the magnetization variation if it remains parallel to the considered direction. The dashed curve corresponds to effects of defects on the wall motion similar to those observed along the easy-magnetization direction.

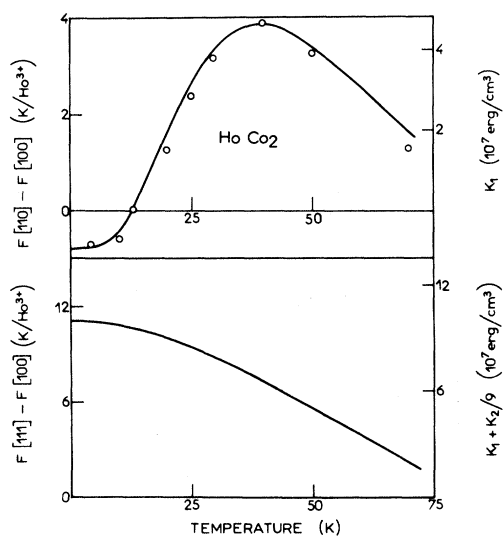


FIG. 5. Thermal variation of the free-energy differences  $F[110]-F[100]$  and  $F[111]-F[100]$  for  $\text{HoCo}_2$ . Round points represent the experimental values. Full lines represent the thermal variations calculated with the parameters values  $x = -0.4687$ ,  $W = 0.6$  K, and  $\alpha = 28$  K.

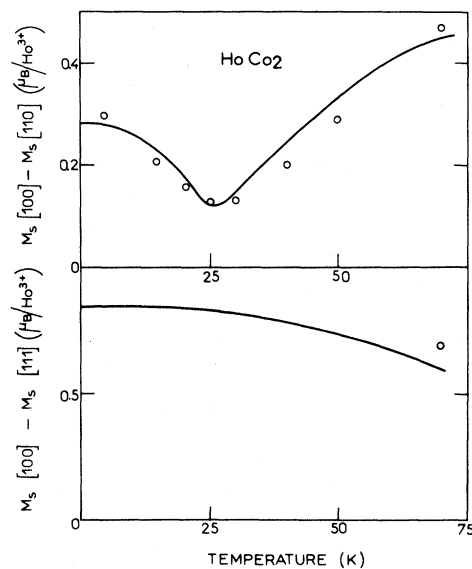


FIG. 6. Thermal variations of the  $\text{HoCo}_2$  magnetization anisotropy. Round points represent the experimental values. Full lines represent the thermal variations calculated with the parameters value  $x = -0.4687$ ,  $W = 0.6$  K, and  $\alpha = 28$  K.

the  $\text{Ho}^{3+}$  ground multiplet may be written

$$\mathcal{H} = \mathcal{H}_c + \mathcal{H}_H.$$

Following the Lea-Leask-Wolf<sup>11</sup> notations, the crystal-field Hamiltonian  $\mathcal{H}_c$  for the cubic symmetry of the ions here considered is

$$\mathcal{H}_c = W[xO_4/F_4 + (1 - |x|)O_6/F_6],$$

where  $W$  is an energy scale factor,  $x$  represents the relative importance of the fourth- and sixth-order terms, and  $O_4$  and  $O_6$  are linear combinations of the Stevens equivalent operators of fourth and sixth order, respectively. These combinations depend on the quantization direction chosen.<sup>12</sup>  $F_4$  and  $F_6$  are factors common to all matrix elements; for  $\text{Ho}^{3+}$ , their values are  $F_4 = 60$  and  $F_6 = 13860$ .<sup>11</sup> The  $W$  and  $x$  parameters are related to the  $B_4$  and  $B_6$  coefficients, describing the fourth- and sixth-order terms of  $\mathcal{H}_c$ , by the relations

$$Wx = B_4 F_4 \quad \text{and} \quad W(1 - |x|) = B_6 F_6.$$

No distortion has been observed by x-ray measurements at low temperature, and magnetostriction effects have been neglected. In a molecular-field model,  $\mathcal{H}_H$  may be written

$$\mathcal{H}_H = \alpha \vec{J} \cdot \vec{u} = g_s \mu_B \vec{J} \cdot \vec{u} (H_m + H_e),$$

where  $H_m$  is the molecular field acting on the ion and  $H_e$  is the external field.  $\vec{u}$  is a unit vector along the quantization direction chosen.

The total Hamiltonian is defined by the three parameters  $W$ ,  $x$ , and  $\alpha$ . To take into account the temperature effects, the energy-level population was calculated by means of Boltzmann statistics, in the same way as done by Atzmony *et al.*<sup>13</sup> in a study of spin reorientations in rare-earth-iron ternary Laves phases. In the calculation of the free energy, the term  $-T \ln Z$ , where  $Z$  is the partition function, is added to the ground-state energy. Diagonalization of the Hamiltonian and calculation of the magnetization, free-energy, and entropy values as a function of the  $W$ ,  $x$ ,  $\alpha$ , and  $T$  parameters were performed by computer. The quantization directions chosen were the three principal symmetry axes:  $[100]$ ,  $[110]$ , and  $[111]$ .

#### A. $\text{HoNi}_2$

In  $\text{HoNi}_2$ , nickel is not magnetic<sup>14</sup>; the  $\alpha$  parameter in zero external field is then defined by the paramagnetic Curie temperature  $\Theta_p = 16$  K and by the spontaneous magnetization  $\sigma_s = 7.55 \mu_B$  at 1.4 K. Its value is  $\alpha = 4.0$  K.  $[100]$  being the easy-magnetization direction, the  $B_4$  coefficient is negative.  $W$  and  $x$  then have opposite signs. These parameters have been determined by searching for the best agreement between calcu-

lated  $M_c$  and measured  $M_0$  values of the magnetization at 1.4 K, as a function of the field applied along the easy-magnetization direction  $[100]$ . Figure 7 shows the residues  $R = 10 \sum (M_c - M_0)^2$  for the best  $W$  and  $x$  coupled values. Only the values of  $x$  in the range  $-0.485$  to  $-1.0$  have been considered because, for  $-0.485 < x < 0.0$ ,  $[110]$  is the easy-magnetization direction, and for  $0.0 < x < 0.19$ ,  $[111]$  is not the hardest one. With  $0.19 \leq x \leq 1.0$ , good residues values can be obtained if  $|W| > 1.0$ ; the calculated magnetizations along the hard-magnetization directions are then too small because of an excessively large splitting of the ground multiplet by the crystal field ( $> 550$  K). In Fig. 2, the observed magnetization curves are compared to those calculated at 1.4 K for  $W = 0.62$  K and  $x = -0.50$  along the three principal axes. The crystal-field effects are more important in  $\text{HoNi}_2$  than the magnetic field effects, and the energy anisotropy increases with the magnetic field. It is therefore impossible to determine from these experiments the field value for which magnetization has become parallel to the  $[110]$  or  $[111]$  direction. The inflection of the calculated magnetization curve along the  $[111]$  direction corresponds to an inversion, caused by the field, between the ground state and the first-excited level. Spontaneous magnetizations measured at various temperatures and those calculated with the parameters defined above are compared in the insert of Fig. 2.

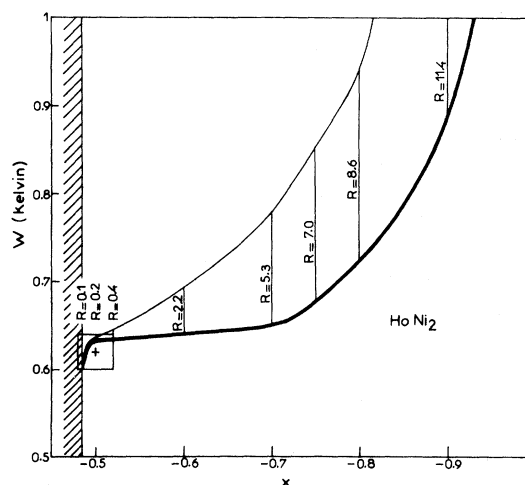


FIG. 7. Variation of the  $\text{HoNi}_2$   $W$  parameter which gives for each value of  $x$  the best agreement between the calculated  $M_c$  ( $\alpha = 4.0$  K) and measured  $M_0$  values of the magnetization at 1.4 K for a field applied along the easy-magnetization direction  $[100]$ . The residues  $R = 10 \sum (M_c - M_0)^2$  are plotted from this curve, parallel to the  $W$  axis.  $R < 0.4$  is obtained for  $W$  and  $x$  values inside the square centered on  $W = 0.62$  K and  $x = -0.50$ .

B. HoCo<sub>2</sub>

In HoCo<sub>2</sub>, cobalt is magnetic. An estimate of the molecular field acting on holmium atoms may be obtained from the paramagnetic reciprocal susceptibility. Two models can explain this variation, one assuming that the cobalt magnetic moment is intrinsic, the other one that it is induced by the interactions due to holmium atoms.<sup>15, 16</sup> Both models lead to the same order of magnitude for the molecular field,  $H_M \approx 400$  kOe, corresponding to the value  $\alpha = 34$  K. At 14 K, the easy magnetization of HoCo<sub>2</sub> changes from the [110] axis to the [100] one as temperature is increased. The ground-state-level energies for these two directions then have close values. Therefore the  $x$  value has to be around  $-0.5$ . A refinement of the different parameters has been done by comparing the thermal variation of the calculated free-energy difference  $F[110] - F[100]$  to that observed from the magnetization curves along the [110] and [100] directions, the cobalt anisotropy and the magnetostriction being negligible. The best agreement was obtained for  $W = 0.60$  K,  $x = -0.4687$ , and  $\alpha = 28$  K ( $H_m = 340$  kOe). The calculated variation is compared to the experimental points on Fig. 5. The variation of the calculated free-energy difference  $F[111] - F[100]$  is also plotted. The values of the anisotropy constants at 0 K are  $K_1 = -10^7$  erg/cm<sup>3</sup> and  $K_2 = 10^9$  erg/cm<sup>3</sup>.

The calculated magnetization differences  $M[100] - M[110]$  and  $M[100] - M[111]$  in a 100-kOe external field are shown in Fig. 6 as a function of temperature. Because of the very high value of the  $K_2$  constant, only the magnetization anisotropy between [100] and [110] directions could be experimentally determined. The obtained values are plotted on the same figure and the agreement is very satisfactory, the cobalt magnetization anisotropy being negligible. The holmium magnetization calculated along the easy-magnetization direction [110] at 4.2 K is  $9.3 \mu_B/\text{Ho}$ . This value compared to the HoCo<sub>2</sub> spontaneous magnetization ( $7.7 \mu_B/\text{HoCo}_2$ ) leads to a magnetic moment of  $0.8 \mu_B/\text{Co}$ , in good agreement with the value determined by neutron diffraction.<sup>17</sup>

The change of easy-magnetization direction at 14 K is associated with a change from one level scheme of the ground multiplet to another one. These two schemes are shown in Fig. 8. An entropy discontinuity of  $1.6 \text{ JK}^{-1} \text{ mole}^{-1}$  at the transition was calculated, corresponding to a change in the level population. A latent heat is associated with this entropy gap, leading to a specific-heat anomaly. Such an anomaly has been recently observed at 15 K by Voiron,<sup>4</sup> the entropy gap deduced from the specific-heat measurements being  $1.4$

$\text{JK}^{-1} \text{ mole}^{-1}$ . We have measured the thermal variation of the specific heat of the button from which the single-crystalline sphere was extracted, and the specific-heat anomaly is found at 13.6 K. This difference between the anomaly temperatures is due to the first-order character of the transition. Stoichiometry shifts, related to the method of preparation, may involve slight variations of the  $x$  parameter, which precisely defines the transition temperature.

## V. CONCLUSION

Crystal-field effects on the Ho<sup>3+</sup> ions explain well the magnetization mechanisms below the ordering temperature although rare-earth atoms are on a high-symmetry site ( $T_d$ ). These effects in the  $R\text{Ni}_2$  compounds had already been calculated in 1963 by Bleaney<sup>18</sup> with a point-charge model. Signs of fourth- and sixth-order terms deduced from magnetization measurements are identical to those calculated by Bleaney, but the order of magnitude of these terms is found to be much higher. The different values obtained for HoNi<sub>2</sub> and HoCo<sub>2</sub> are reported in Table I. Fourth- and sixth-order-term values are nearly independent of the transition metal alloyed. Nickel, having a full 3d band, is not magnetic; its charge is null.

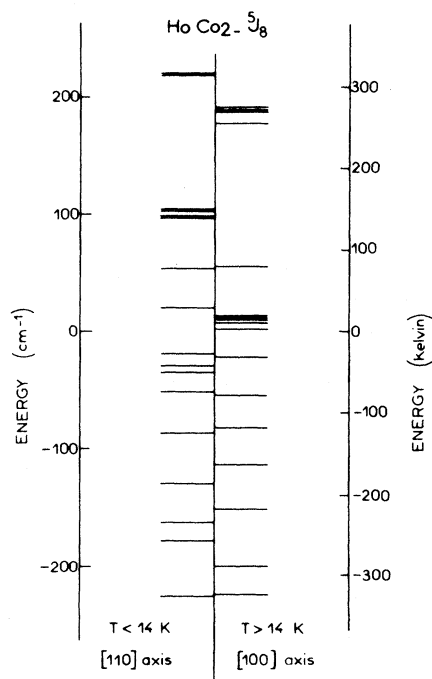


FIG. 8. Splitting of the  $^5J_8$  ground multiplet of the Ho<sup>3+</sup> ion in HoCo<sub>2</sub> on both sides of the change of easy-magnetization direction calculated with the parameter values  $x = -0.4687$ ,  $W = 0.6$  K, and  $\alpha = 28$  K.

TABLE I. Comparison of crystal-field parameters of  $\text{HoNi}_2$  and  $\text{HoCo}_2$  determined from magnetization measurements to those calculated in a point-charge model.  $\Delta$  represents the total splitting of the ground multiplet by the crystal field.

		$W$ (K)	$x$	$10^4 B_4$ (K)	$10^4 B_6$ (K)	$\Delta$ (K)
$\text{HoNi}_2$	Point-charge model	0.084	-0.783	-11.0	1.3	50.5
	Experimental results	0.62	-0.5	-51.7	22.4	281.4
$\text{HoCo}_2$	Point-charge model	0.082	-0.785	-10.7	1.3	49.4
	Experimental results	0.6	-0.4687	-46.9	23.0	267.8

The cobalt moment is  $0.8\mu_B$  in  $\text{HoCo}_2$ , which approximately corresponds to a  $3d^9$  electronic configuration, i.e., a zero charge as for nickel. The contribution of crystal-field effects on  $5d$  electrons may influence the fourth-order terms.<sup>19</sup>

These crystal-field effects lead to giant magnetocrystalline anisotropies for the rare-earth ions, already found in  $R\text{Fe}_2$  Laves phases by Clark *et al.*<sup>20</sup> From experimental results obtained on a  $\text{ErFe}_2$  single crystal,<sup>20</sup> the magnetocrystalline anisotropy constants  $K_1$  and  $K_2$  have been calculated using a scaling law for various  $R\text{Fe}_2$  compounds by Dariel and Atzmony.<sup>21</sup> The high values that we have found have the same order of magnitude as those calculated for  $\text{HoFe}_2$ .

Because the cobalt anisotropy measured in  $\text{GdCo}_2$  is negligible, the change of easy-magnetization direction is not due to a competition between opposite-sign anisotropies on cobalt and rare earth, as in  $R\text{Co}_5$  compounds.<sup>22</sup> It corresponds to a change due to the temperature from one energy level scheme to another. The transi-

tion is of first order; an entropy discontinuity is associated with it, leading to a specific-heat anomaly. In the Callen and Callen model,<sup>23</sup> this change of easy-magnetization direction can be considered as the result of a temperature decrease of the anisotropy coefficients which is stronger for the sixth order than for the fourth order. The bump observed on the thermal variations of the magnetization of a polycrystalline sample in a constant field is associated with the zero value of the  $K_1$  anisotropy constant at the transition. In  $\text{HoNi}_2$ , exchange interactions are weak compared to crystal-field effects; the anisotropy increases so much with the applied magnetic field that it is no longer possible to measure it. The Curie temperature of  $\text{HoCo}_2$  is of first order; the thermal variation of the transition field does not depend on the direction of the applied field. This result confirms the origin of the transition which must be associated with a change of the cobalt electronic configuration<sup>3</sup> and not to crystal-field effects on the  $\text{Ho}^{3+}$  ions.

<sup>1</sup>B. Bleaney, *Rare Earth Research II* (Gordon and Breach, New York, 1963), p. 499.

<sup>2</sup>R. Lemaire, *Cobalt* **33**, 201 (1966).

<sup>3</sup>R. Lemaire, D. Paccard, R. Pauthenet, and J. Schweizer, *J. Appl. Phys.* **39**, 1092 (1968).

<sup>4</sup>J. Voiron, thesis (Grenoble University, 1973) (unpublished).

<sup>5</sup>D. Gignoux, F. Givord, and R. Perrier de la Bathie (unpublished).

<sup>6</sup>J. Farrell and W. E. Wallace, *Inorg. Chem.* **5**, 105 (1966).

<sup>7</sup>E. Burzo and J. Laforest, *Int. J. Magn.* **3**, 171 (1972).

<sup>8</sup>E. W. Collings, R. D. Smith, and R. G. Lecander, *J. Less-Comm. Met.* **18**, 251 (1969).

<sup>9</sup>L. Neel, *J. Phys. Radiat.* **5**, 241 (1944).

<sup>10</sup>D. Bloch, F. Chaisse, F. Givord, J. Voiron, and E. Burzo, *J. Phys. C* **32**, 659 (1971).

<sup>11</sup>K. R. Lea, M. J. M. Leask, and W. P. Wolf, *J. Phys. Chem. Solids* **23**, 1381 (1962).

<sup>12</sup>M. T. Hutchings, *Solid State Phys.* **16**, 227 (1966).

<sup>13</sup>U. Atzmony and M. P. Dariel, *Phys. Rev. B* **7**, 4220 (1973).

<sup>14</sup>E. A. Skrabek and W. E. Wallace, *J. Appl. Phys.* **34**, 1356 (1963).

<sup>15</sup>E. Burzo, *Phys. Rev. B* **6**, 2882 (1972).

<sup>16</sup>D. Bloch and R. Lemaire, *Phys. Rev. B* **2**, 2648 (1970).

<sup>17</sup>W. C. Koehler, R. M. Moon, and J. Farrell, *J. Appl. Phys.* **36**, 978 (1965).

<sup>18</sup>B. Bleaney, *Proc. R. Soc. A* **276**, 28 (1963).

<sup>19</sup>H. C. Chow, *Phys. Rev. B* **7**, 3404 (1973).

<sup>20</sup>A. E. Clark, H. S. Belson, and N. Tamagawa, *Phys. Lett. A* **42**, 160 (1972).

<sup>21</sup>M. P. Dariel and U. Atzmony, *Int. J. Magn.* **4**, 213 (1973).

<sup>22</sup>B. Barbara, D. Gignoux, D. Givord, F. Givord, and R. Lemaire *Int. J. Magn.* **4**, 77 (1973).

<sup>23</sup>H. B. Callen and E. Callen, *J. Phys. Chem. Solids* **27**, 1271 (1966).